Multimode Masers of Thermally Polarized Nuclear Spins in Solution NMR

Vineeth Francis Francis Thalakottoor Jose Chacko, Alain Louis-Joseph, Daniel Abergel

▶ **To cite this version:**

Vineeth Francis Francis Thalakottoor Jose Chacko, Alain Louis-Joseph, Daniel Abergel. Multimode Masers of Thermally Polarized Nuclear Spins in Solution NMR. Physical Review Letters, 2024, 133 (15), pp.158001. 10.1103/PhysRevLett.133.158001 . hal-04753220

HAL Id: hal-04753220
https://hal.science/hal-04753220v1

Submitted on 25 Oct 2024

HAL is a multi-disciplinary open access archive for the deposit and dissemination of scientific research documents, whether they are published or not. The documents may come from teaching and research institutions in France or abroad, or from public or private research centers.

L'archive ouverte pluridisciplinaire **HAL**, est destinée au dépôt et à la diffusion de documents scientifiques de niveau recherche, publiés ou non, émanant des établissements d'enseignement et de recherche français ou étrangers, des laboratoires publics ou privés.

Supplementary Material - Multi-mode masers of thermally polarized nuclear spins in solution NMR

Vineeth Francis Thalakottoor Jose Chacko,[1,*] Alain Louis-Joseph,[2,†] and Daniel Abergel[1,‡]

[1] *Laboratoire des Biomolécules, LBM, Département de Chimie, Ecole Normale Supérieure, PSL University, Sorbonne Université, CNRS, 75005 Paris, France*

[2] *Laboratoire de Physique de la Matière Condensée, UMR 7643, CNRS, École Polytechnique , IPP 91120 Palaiseau, France*

I. STABILITY ANALYSIS OF THE MAXWELL-BLOCH EQUATIONS

The dynamics of the magnetization is examined by first determining the fixed points (the stationary solution of $\frac{d\mathbf{m}}{dt} = 0$) and then analyzing the stability of the linearized system in their vicinity.[1] These fixed points have been found in the case where $\omega_1 = 0$, and it was shown that for certain values of the relaxation and feedback field parameters, the (m^2, m_z) system admits an out of thermal equilibrium stable fixed point.[2, 3] that can be a stable focus, meaning that the trajectory of $(m^2(t), m_z(t))$ spirals inwards towards its asymptotic value (see Eqs SM-2-SM-7 in the SI). This motion exactly represents a series of maser pulses with a monotonous decrease of their intensities. This discussion[2, 4] is summarized below.

Denoting $m_t = m_x + im_y = \sqrt{u}e^{i\phi(t)}$, the MB equations become:

$$\begin{cases} \dot{u}(t) = 2(\lambda m_z(t)\sin\psi - \gamma_2)u(t) \\ \dot{m}_z(t) = -\lambda\sin\psi u(t) - \gamma_1(m_z(t) - m_0) \\ \dot{\phi}(t) = -\delta + \lambda\cos\psi\ z \end{cases} \tag{SM-1}$$

The fixed points are thus $F_1 = (0, m_0)^t$ and $F_2 = (-\frac{\gamma_1}{\lambda\sin\psi}\left[\frac{\gamma_2}{\lambda\sin\psi} - m_0\right], \frac{\gamma_2}{\lambda\sin\psi})^t$, and their stability dictates the dynamics of the system. An analysis shows that, depending on the parameters, one of F_1 and F_2 is stable and the other is unstable. Thus, when the product $m_0 \times \sin\psi < 0$, F_2 is unstable and F_1 is stable. This corresponds to the usual radiation damping case, where the radiation feedback field from the probe drives the magnetization towards $+z$. In contrast, for $m_0 \times \sin\psi > 0$, two situations occur and F_2 is stable if the condition $\lambda\sin\psi m_0 - \gamma_2 > 0$ is fulfilled. When in addition $\Delta = \gamma_z(\gamma_z + 8\gamma_2 - 8\lambda m_0\sin\psi)$, then F_2 is a focus. This describes the evolution of a sustained maser towards a stationary magnetization that precesses about the z axis on a cone of semi-angle α such that $\tan\alpha = \frac{\lambda\sin\psi\sqrt{u}}{\gamma_2}$. The physical interpretation of the necessary condition $m_0 \times \sin\psi > 0$ for such dynamics to occur is the existence of two competing processes originating from the feedback field and longitudinal relaxation.

A. Fixed points of the linearized Maxwell-Bloch equations

Linearization at:

$$F_2 = (-\frac{\gamma_z}{\lambda\sin\psi}\left[\frac{\gamma_2}{\lambda\sin\psi} - m_0\right], \frac{\gamma_2}{\lambda\sin\psi}, m_0) \tag{SM-2}$$

$$\begin{bmatrix} \dot{U} \\ \dot{Z} \\ \dot{W} \end{bmatrix} = \begin{bmatrix} 0 & 2\lambda\sin\psi\ u^{st} & 0 \\ -\lambda\sin\psi & -\gamma_z & \gamma_z \\ 0 & 0 & -\gamma_{st} \end{bmatrix} \begin{bmatrix} U \\ Z \\ W \end{bmatrix} + \begin{bmatrix} -2\lambda\sin\psi ZU \\ 0 \\ 0 \end{bmatrix} \tag{SM-3}$$

* vineeth.thalakottoor@ens.psl.eu

† alain.louis-joseph@polytechnique.edu

‡ daniel.abergel@ens.psl.eu

The eigenvalues are:

$$\begin{aligned} x_0 &= -\gamma_{st} \\ x_\pm &= \frac{-\gamma_z \pm \sqrt{\Delta}}{2},\ \Delta = \gamma_z(\gamma_z + 8\gamma_2 - 8\lambda m_0 \sin\psi) \end{aligned} \tag{SM-4}$$

Now, if the condition $m_0 \times \sin\psi < 0$ then one has: $\Delta >$ and $x_+ > 0,\ x_- < 0$

Linearization at:

$$F_1 = (0, m_0, m_0) \tag{SM-5}$$

$$\begin{aligned} \begin{bmatrix} \dot{U} \\ \dot{Z} \\ \dot{W} \end{bmatrix} &= \begin{bmatrix} 2(\lambda\sin\psi - \gamma_2) & 0 & 0 \\ -\lambda\sin\psi & -\gamma_z & \gamma_z \\ 0 & 0 & -\gamma_{st} \end{bmatrix} \begin{bmatrix} U \\ Z \\ W \end{bmatrix} \\ &+ \begin{bmatrix} -2\lambda\sin\psi ZU \\ 0 \\ 0 \end{bmatrix} \end{aligned} \tag{SM-6}$$

$$\begin{aligned} x_0 &= -\gamma_{st} \\ x_1 &= -\gamma_z \\ x_2 &= 2(\lambda\sin\psi m_0 - \gamma_2) \end{aligned} \tag{SM-7}$$

B. Fixed point stability

- Fixed point stability in the case $m_0 \times \sin\psi < 0$. This corresponds to the radiation damping case. In this case, one has:
  - If $\Delta >$ and $x_+ > 0,\ x_- < 0$
- Fixed point stability in the case $m_0 \times \sin\psi > 0$
  - if $\lambda\sin\psi m_0 - \gamma_2 > 0$ then $x_2 > 0$ and F_1 is unstable, and F_2 is stable.
    - If in addition $\Delta < 0$, then F_2 is a stable focus.
  - If $0 < \lambda\sin\psi m_0 < \gamma_2$, then $x_2 < 0$ and F_1 is stable, and F_2 is unstable.

II. LIMIT CASES OF EQ.??

The nonlinear dynamical system of Equations **??** can essentially be investigated by numerical simulations. To this aim equations can be reformulated, as proposed in ref.[5] (or in Equation SM-1 above[2]), by introducing the amplitudes and phases $a_k(t)$ and $\phi_k(t)$ of each moment $m_k(t)$: $m_k(t) = a_k(t)e^{i\phi_k(t)}$. The evolution of one of the moments $\mathbf{m}_i$ due to the effect of the feedback field is thus:

$$\begin{aligned} \dot{m}_i &= -(i\delta\omega_i + \gamma_{2i})m_i - i\omega_1 m_{zi} e^{i\psi_1} + i\gamma G m_{zi} e^{-i\psi} \sum_k a_k e^{i\phi_k} \\ \dot{m}_{zi} &= -\omega_1 \mathcal{R}e(ie^{-i\psi_1} m_i) - \gamma_{1i}(m_{zi} - m_{z0i}) - \gamma G a_i \sum_k a_k \sin(\phi_i - \phi_k + \psi) \end{aligned} \tag{SM-8}$$

and the differential equations for the amplitudes and phases are thus:

$$\begin{aligned} \dot{a}_i &= -\gamma_{2i} a_i + \omega_1 m_{zi} \sin(\phi_i + \psi_1) + \gamma G m_{zi} \sum_k a_k \sin(\phi_i - \phi_k + \psi) \\ \dot{\phi}_i &= \delta\omega_i + \frac{\omega_1}{a_i} m_{zi} \cos(\phi_i + \psi_1) - \frac{\gamma G m_{zi}}{a_i} \sum_k a_k \cos(\phi_i - \phi_k + \psi) \\ \dot{m}_{zi} &= \omega_1 a_i \sin(\phi_i + \psi_1) - \gamma_{1i}(m_{zi} - m_{z0i}) - \gamma G a_i \sum_k a_k \sin(\phi_i - \phi_k + \psi) \end{aligned} \tag{SM-9}$$

In general, equations SM-9 can only be studied by numerical simulations. Nevertheless, qualitative results can be obtained in two limiting cases, when $\omega_1 = 0$. First, assume that all the moments $m_k(t)$ have nearly identical Larmor frequencies $\delta\omega_k = \delta\tilde{\omega}$, and relaxation rates $\gamma_{1,2}$. Then, from Equation SM-8, one has:

$$\dot{m}(t) = -i\delta\tilde{\omega}\sum_i m_i(t) - \gamma_2\sum_i m_i(t) + i\gamma G e^{i\psi}\sum_i m_{zi}(t)\sum_k m_k(t) \tag{SM-10}$$

$$= -(i\delta\tilde{\omega} + \gamma_2)m(t) + i\gamma G e^{i\psi} m_z(t)m(t) \tag{SM-11}$$

In the case where all pairwise resonance frequency differences $|\delta\omega_i - \delta\omega_k|$ are large, and so are the differences $|\phi_i(t) - \phi_k(t)|$, then the functions $\sin(\phi_i(t) - \phi_k(t) - \psi)$ and $\cos(\phi_i(t) - \phi_k(t) - \psi)$ are fast varying functions of the time as compared to the amplitudes $a_k(t)$and $m_{zk}(t)$ components of the moments, for all $k \neq i$. Therefore, the average $\bar{a}_i = \dfrac{1}{\Delta t}\displaystyle\int_{t_0}^{t_0+\Delta t} A(\tau)d\tau$ obeys the following relations:

$$\begin{aligned}
\Delta t\bar{a}_i &= \int_{t_0}^{t} -\gamma_{2i}a_i - \gamma G m_{zi}\sum_k a_k\cos(\phi_i - \phi_k - \psi)d\tau \\
&\approx -\int_{t_0}^{t}\left[\gamma_{2i}a_i + \gamma G\cos\psi\, m_{zi}(\tau)a_i(\tau)\right]d\tau - \gamma G\sum_{k\neq i} m_{zi}(t)a_k(t)\int_{t_0}^{t}\cos(\phi_i - \phi_k - \psi)d\tau \qquad \text{(SM-12)} \\
&\approx -\int_{t_0}^{t}\left[\gamma_{2i}a_i + \gamma G m_{zi}(\tau)a_i(\tau)\right]d\tau
\end{aligned}$$

Similarly, one obtains for the moving averages $\bar{\phi}_i$ and $\bar{m}_{zi}$ the following equations:

$$\Delta t\bar{\phi}_i(t) \approx \int_{t_0}^{t}\left[\delta\omega_i + \gamma G m_{zi}(t)\sin\psi\right]d\tau \tag{SM-13}$$

$$\Delta t\bar{m}_{zi}(t) \approx \int_{t_0}^{t}\left[-\gamma_{1i}(m_{zi} - m_{z0i}) + \gamma G\bar{a_i^2}(\tau)\cos(\psi)\right]d\tau \tag{SM-14}$$

Thus, the dynamics of the component $\mathbf{m}_i(t)$ obeys the approximate evolution equations:

$$\dot{\bar{a}}_i(t) = -\gamma_{2i}\bar{a}_i - \gamma G m_{zi}(t)\bar{a}_i(t) \tag{SM-15}$$

$$\dot{\bar{m}}_{zi}(t) = -\gamma_{1i}(\bar{m}_{zi} - m_{z0i}) + \gamma G\bar{a_i^2}(t)\cos(\psi) \tag{SM-16}$$

$$\dot{\bar{\phi}}_i(t) = \delta\omega_i + \gamma G\bar{m}_{zi}(t)\sin\psi \tag{SM-17}$$

This therefore shows that in this case of large offset separations, the moving average for the magnetization $\mathbf{m}_i(t)$ again obeys Maxwell-Bloch equations, and each $\mathbf{m}_i(t)$ is decoupled from all other $\mathbf{m}_k(t)$.

III. REFERENCE SPECTRA OF METHANOL AND ETHANOL (FIGURE SM-1)

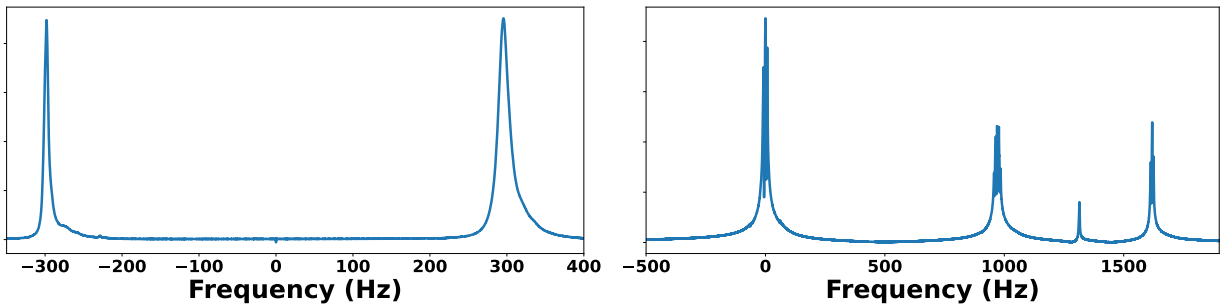

(a) (b)

FIG. SM-1. Reference Spectra of Methanol (a) and Ethanol (b). Frequencies are labelled with the LO as the reference. Spectra were acquired at 9.4 T. For the methanol, the lines are unresolved due to the addition of $CuSO_4$ in the solution.

IV. INSTRUMENTATION: THE ELECTRONIC FEEDBACK CONTROL UNIT (EFCU)

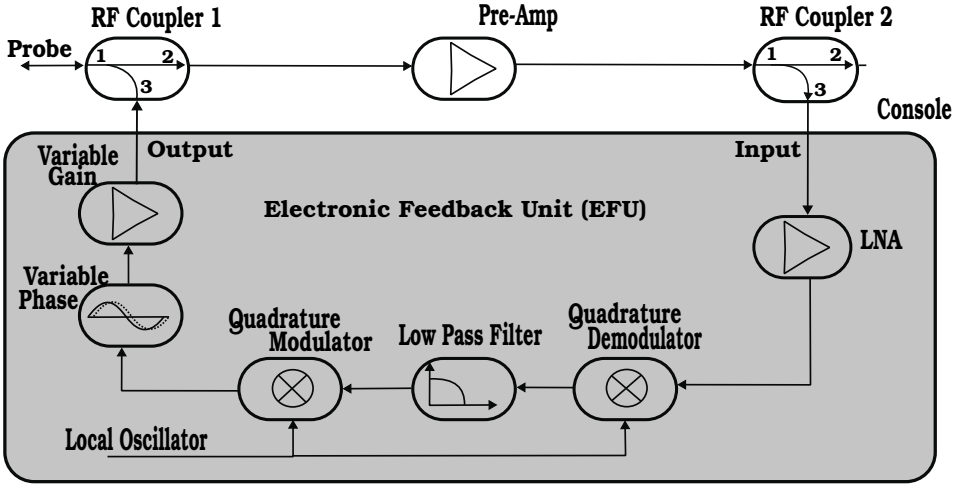

FIG. SM-2. Electronic Feedback Control Unit (eFCU)- The signal from the probe is picked up at the output of the preamplifier through the directional coupler "2" and amplified by a low-noise amplifier (+20 dB gain). Demodulation at 400 MHz (local oscillator - LO) was used for sake of filtering, and picked up from the ^{1}H power amplifier of the spectrometer. Its power set to a 14.7 dBm. The re-modulated signal is then adjusted in phase and gain before being re-injected into the probe through the rf coupler 1. Gain adjustment was performed by a +20 dB low noise amplifier and a set of variable attenuators in the range 0 to 111 dB.

A fraction of the induction signal is picked up at the output of the preamplifier through a directional coupler and amplified through a low-noise amplifier. This signal is then demodulated using a 400 MHz local oscillator (LO) reference generated from the ^{1}H power amplifier of the spectrometer. The resulting in-phase and quadrature demodulated signals are fed into a low-pass filter of bandwidth 100 kHz and re-modulated at the proton Larmor frequency. The filter bandwidth can be adjusted between 100 Hz and 100 kHz, depending on the application. After re-modulation the radiofrequency signal is phase adjusted by a voltage-controlled phase modulator, and the gain of the eFCU output signal was controlled using a second LNA (+20 dB) and a set of variable attenuators in the range 0 to 111 dB (with a minimum attenuation step of 0.1 dB). The LO was switched on throughout acquisition. Finally, the phase- and gain-adjusted signal is fed back into the probe via an additional directional coupler. The rf leakage of the LO from the mixers of the eFCU is first minimized ($\lesssim 2$ mV) by adjusting the offset voltage at the input of the low-pass filter.

Mirror images that are symmetric with respect to the demodulation frequency are caused by the low pass filtering of the signal that requires a demodulation/remodulation stage of the audio signal in the eFCU. Demodulation of the input signal $\nu_0 + \nu$, where ν_0 is the LO radiofrequency and $\nu = \delta\omega/2\pi$ is the audiofrequency of the spin, yields signals at $2\nu_0 + \nu$ and ν. The former is filtered out by the eFCU low-pass filter, and the latter gives signals at $\nu_0 \pm \nu$ after re-modulation with the same LO frequency ν_0. The small and constant rf leakage yields a spike in the spectrum at the LO frequency. These features are illustrated in Fig. SM-3.

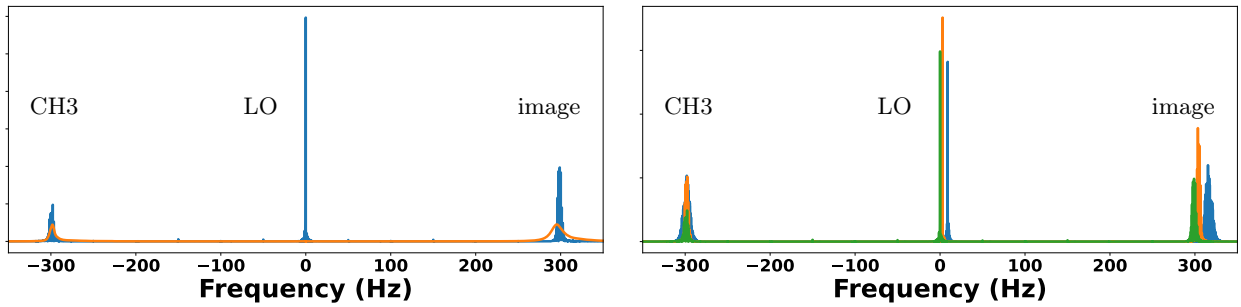

(a) (b)

FIG. SM-3. Effect of modifications of the modulation/demodulation reference frequency (LO) on the methanol resonance line in maser experiments - Spectra of a methanol maser from CH3 for different LO positions. In (a): a maser spectrum (blue) is superimposed with a reference FID (orange); the zero frequency corresponds to he LO position for the spectrum on the left. In (b): Changing the LO frequency only changes the image location whilst the CH3 resonance line remains fixed. The carrier frequency is the same for all experiments.

V. MEASUREMENT OF THE RF LEAKAGE (FIGURE SM-4)

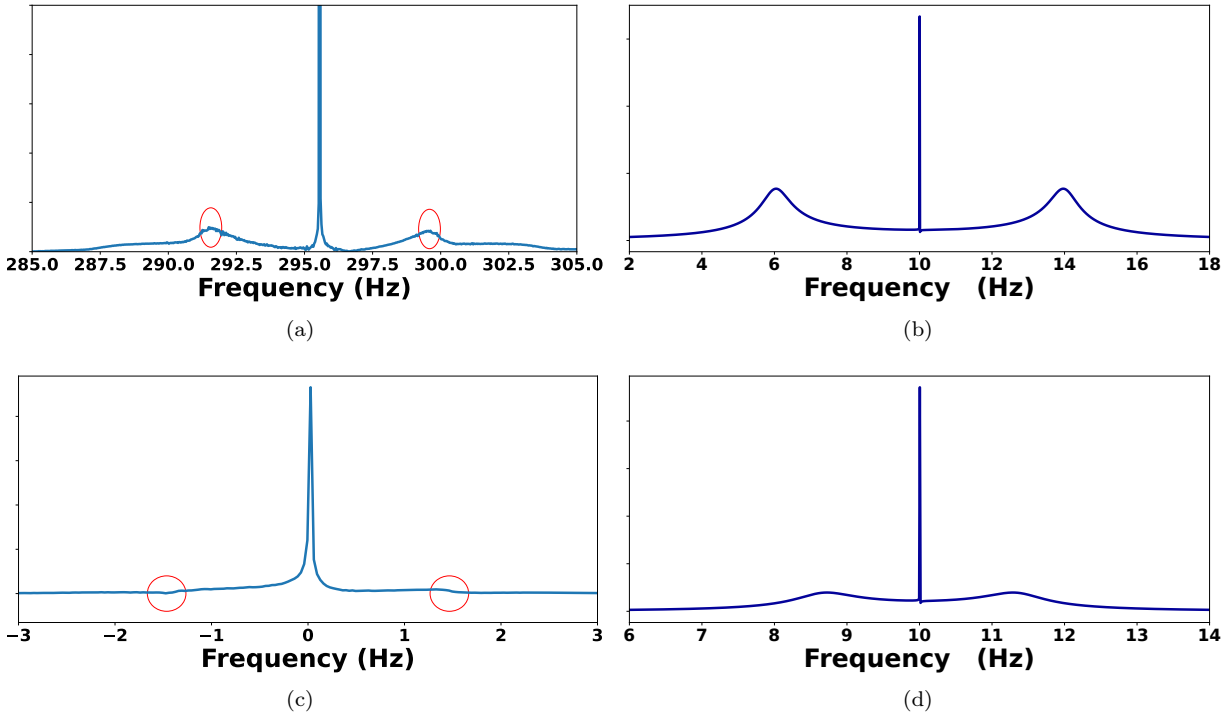

(a) (b)

(c) (d)

FIG. SM-4. Measurement of the rf leakage from the eFCU by a nutation experiment. Figure (a) and (c) are the magnitude spectra corresponding to methanol and ethanol when the LO was set on the CH3 resonance whilst the input of eRFCU was disconnected from the probe during acquisition. Two peaks corresponding to the nutation of the spins and caused by the constant rf leakage were respectively observed at $\nu_1 = 4$ Hz and $\nu_1 = 1.4$ Hz away from the Larmor frequency of CH3 in methanol and ethanol. A simulation was performed using rf leakage amplitude of 4 Hz and 1.4 Hz with frequency 10 Hz with out radiation damping are shown in figures (b) and (d).

VI. SPECTRAL CLUSTERING IN THE THREE-MODE ETHANOL MASER (FIG. SM-5)

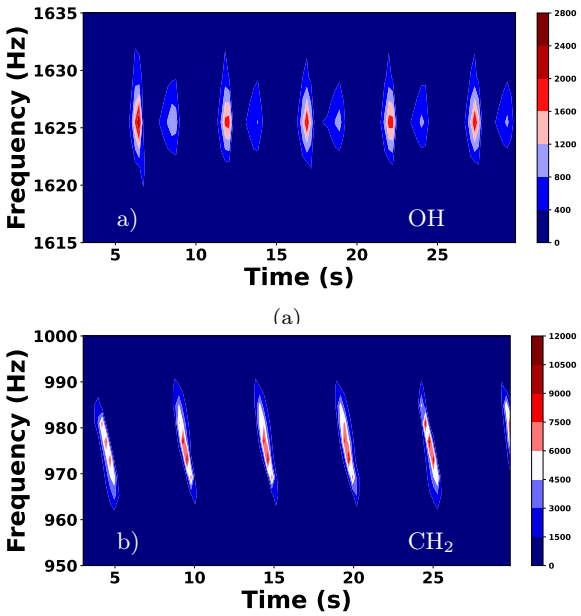

FIG. SM-5. Spectral clustering in the three-mode ethanol maser. The time envelopes shows a succession of pairs of maser pulses in a narrow frequency band for OH (5(a)), and several maser components shifted in time for CH_2 (5(b)).

VII. SPECTRAL CLUSTERING IN ETHANOL: A TOY MODEL VERSUS EXPERIMENT (FIG. SM-6)

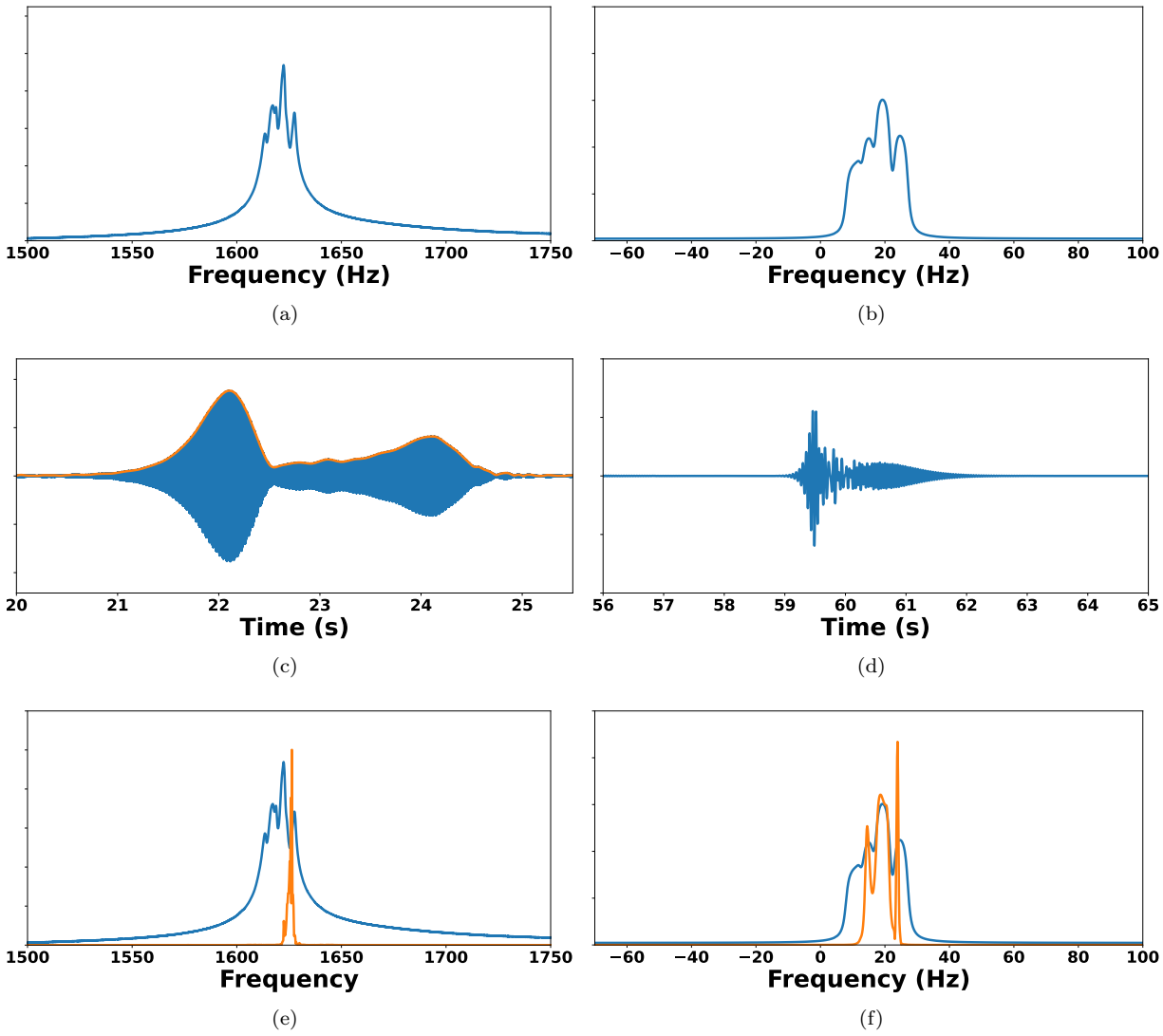

FIG. SM-6. Maser spectral clustering in ethanol: a toy model simulation versus experiment. Left column - Figure (a)corresponds to the spectrum of the OH multiplet acquired after a 90^o pulse in the absence of eFBU. In (c): single burst from the experimental maser signal shown in figure **??** of the article. In (e), the spectrum in (a) and the Fourier transforms of (c) show the spectral clustering. Right column - A simulation was performed with five sets of 420 spins separated by 0.01 Hz centered at 10 Hz, 14 Hz, 15.5 Hz, 19.5 Hz and 25 Hz with $m_o = 0.002, 0.0014, 0.0014, 0.004, 0.003$ to simulate a mock OH multiplet. The associated spectrum and a single burst of the simulated maser signal are shown in (b) and (d), respectively. In (f) the spectral clustering from the simulation is shown.

VIII. STRUCTURE OF THE METHANOL SPECTRUM (FIG.??)

The Ш_T function, defined as:

$$\text{Ш}_T = \sum_{n=-\infty}^{\infty} \delta(t - nT) \tag{SM-18}$$

has the Fourier transform:

$$\text{Ш}_{1/T} = \frac{1}{T} \sum_{n=-\infty}^{\infty} \delta(\nu - \frac{n}{T}) \tag{SM-19}$$

The induction signal of Fig.**??** can be approximately represented as the sum of two periodic signals of the same period T. Suppose f and g denote the shape of the signal over one period T and zero elsewhere. If in addition g is shifted in time, then the signal can be represented as:

$$S(t) = (f(t) + g(t + \Delta)) * \text{Ш}_T(t) \tag{SM-20}$$

with $\Delta < T$. The Fourier transform of this signal is thus:

$$S(f) = \frac{1}{T} \left[\hat{f}(\nu) + e^{-2i\pi\Delta\nu} \hat{g}(\nu) \right] \text{Ш}_{1/T}(\nu) \tag{SM-21}$$

Now suppose that $g(t) = Af(t)$, $A > 0$, and $\Delta = T/2$. The spectrum becomes:

$$\begin{aligned} S(f) &= \frac{1}{T} \hat{f}(\nu) \left[1 + Ae^{-2i\pi\nu T/2} \right] \text{Ш}_{1/T}(\nu) \\ &= \frac{1}{T} \sum_{n=-\infty}^{\infty} \hat{f}(n/T) \left[1 + Ae^{-i\pi n} \right] \end{aligned} \tag{SM-22}$$

This shows that the coefficient of $\hat{f}(n/T)$ is equal to $1 \pm A$, depending whether n is even or odd. Therefore, the spectral lines are alternatively larger or smaller than the spectrum f. This phenomenon explains the kind of spectrum with alternating intensities observed in Fig.**??** of the article.

---

[1] J. Guckenheimer and P. Holmes, *Nonlinear Oscillations, Dynamical Systems, and Bifurcations of Vector Fields*, Applied Mathematical Sciences No. 42 (Springer, 1983).

[2] D. Abergel, A. Louis-Joseph, and J.-Y. Lallemand, Self-sustained Maser oscillations of a large magnetization driven by a radiation damping-based electronic feedback, The Journal of Chemical Physics **116**, 7073 (2002), https://pubs.aip.org/aip/jcp/article-pdf/116/16/7073/10838953/7073_1_online.pdf.

[3] D. Abergel, V. Thalakottoor, and A. Louis-Joseph, An nmr spectroscopist's view of nonlinear magnetization dynamics: in liquid and frozen solutions, at high and low temperatures, at low and high polarizations, in *From the nonlinear dynamical systems theory to observational chaos* (2023).

[4] E. M. M. Weber, D. Kurzbach, and D. Abergel, A dnp-hyperpolarized solid-state water nmr maser: observation and qualitative analysis, Phys. Chem. Chem. Phys. **21**, 21278 (2019).

[5] S. Appelt, S. Lehmkuhl, S. Fleischer, B. Joalland, N. M. Ariyasingha, E. Y. Chekmenev, and T. Theis, Sabre and phip pumped raser and the route to chaos, Journal of Magnetic Resonance **322**, 106815 (2021).